BMC Genomics

RESEARCH

Open Access

Analysis and identification of mitochondria-related genes associated with age-related hearing loss

Tianyu Ma[1], Xiaoyun Zeng[1], Mengting Liu[1], Shijia Xu[1], Yuyao Wang[1], Qilong Wu[1] and Tianhong Zhang[1*]

Abstract

Background To explore the mitochondrial genes that play a key role in the occurrence and development of age-related hearing loss (ARHL) and provide a basis for the study of the mechanism of ARHL.

Results 503 differentially expressed genes (DEGs) were detected in the GSE49543 dataset. 233 genes were up-regulated, and 270 genes were down-regulated. There are 1140 genes in the mitochondrial gene bank, and 28 differentially expressed genes related to ARHL. These genes are mainly involved in mitochondrial respiratory chain complex assembly, small molecule catabolism, NADH dehydrogenase complex assembly, organic acid catabolism, precursor metabolites and energy production, and mitochondrial span Membrane transport, metabolic processes of active oxygen species. Then, Cytoscape software identified the three key genes: Aco2, Bcs1l and Ndufs1. Immunofluorescence and Western blot experiments confirmed that the protein content of three key genes in aging cochlear hair cells decreased.

Conclusion We employed bioinformatics analysis to screen 503 differentially expressed genes and identified three key genes associated with ARHL. Subsequently, we conducted in vitro experiments to validate their significance, thereby providing a valuable reference for further elucidating the role of mitochondrial function in the pathogenesis and progression of ARHL.

Keywords ARHL, Mitochondrial-related genes, Mitochondrial homeostasis

Introduction

Age-related hearing loss (ARHL) is a degenerative condition affecting the cochlea and vestibule, commonly associated with aging [1]. It is characterized by progressive and irreversible bilateral symmetrical sensorineural hearing impairment. Deafness can result in diminished social functioning and a heightened risk of dementia, anxiety, and depression among older individuals, significantly jeopardizing their physical and mental well-being while imposing a substantial burden on both families and society [2, 3]. Due to the unknown etiology of ARHL, treatment primarily relies on hearing aids as there are currently no effective preventive or therapeutic measures available. Recent research advancements have suggested that mitochondrial homeostasis imbalance may be implicated in the development of ARHL [4].

Within cells, mitochondria play a crucial role in regulating oxidative metabolism and serve as the primary source of Reactive Oxygen Species (ROS). Mitochondrial dysfunction serves as an indicator of cellular aging.

*Correspondence:
Tianhong Zhang
zth3856@126.com
[1]The First Affiliated Hospital of Harbin Medical University, No. 23 Youzheng Street, Harbin, Heilongjiang Provice, China

Excessive ROS production during cellular aging results in the loss of mitochondrial membrane potential, an increase in mitochondrial mass, alterations to the mitochondrial respiratory complex, release of cytochrome C, reduction in mitochondrial transcription factor A levels, and an accumulation of fragmented mitochondrial DNA. These events ultimately lead to impaired mitochondrial function and subsequent activation of the apoptotic pathway within mitochondria, which leads to cell senescence and death [5, 6]. Among these, mitochondria-related genes play a crucial role in regulating the production and deficiency of reactive oxygen species (ROS) and are also the primary target of excessive ROS [7, 8]. Mutations and deletions within mitochondria related genes can induce apoptosis and contribute to age-related diseases [9]. To date, over 150 mitochondria-related gene deletions associated with various diseases have been identified through the Mitomap database dedicated to studying the human mitochondrial genome (http://www.mitomap.org) [10].

Currently, there is no definitive conclusion regarding the alterations and impacts of mitochondria-related genes in the cochlear hair cells in the onset and progression of ARHL. However, the significant role of mitochondria-related genes in cellular aging has compelled researchers to give it due attention. In this study, we employed bioinformatics methods to investigate the pivotal mitochondria-related gene factors influencing ARHL. Our findings indicate that ACO2, BCS1L, and Ndufs1 are key mitochondrial genes associated with ARHL, which were further validated through in vitro experiments (Fig. 1).

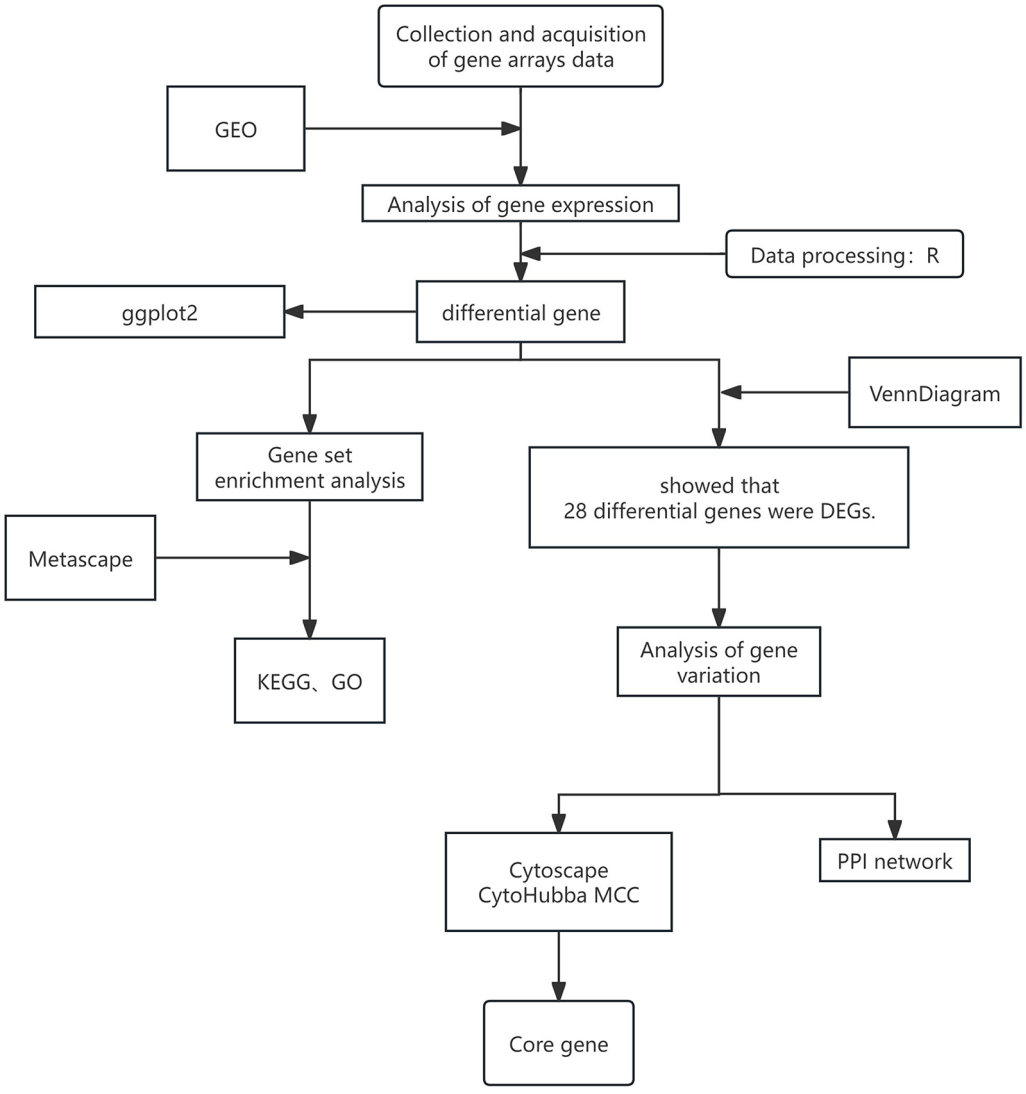

Fig. 1 Flowchart of multi-step analysis based on bioinformatics data

Materials and methods

Collection and acquisition of gene chip data

Access the GEO public database (https://www.ncbi.nlm.nih.gov/geo/) [11]and download the GSE49543 gene chip raw data dataset for research purposes. The GSE49543 dataset comprises gene sequencing data from the cochlea of 40 presbycusis mice, obtained using the GPL339 platform (MOE430A) Affymetrix array. The GEO2R online tool was utilized to standardize the microarray data from the GSE49543 dataset, and a total of 13,661 differentially expressed genes (ARHL-DEGs) were identified using ggplot2 package analysis with a significance threshold of $P<0.05$.

For further investigation, we downloaded Mouse MitoCarta3.0 from Broad Institute's MitoCarta 3.0 database - an inventory of mammalian mitochondrial proteins and pathways that includes a list of 1,136 human and 1,140 mouse protein-coding genes localized on mitochondria [12]. This database provides information on submitochondrial localization and pathway annotation, assigning genes to 149 mitochondrial terms.

Validation of key genes

The accuracy of key genes identified from the GSE49543 dataset was validated using the GEO database. R software (version 4.1.3; https://www.r-project.org/) is a stati stical analysis, graphical visualization, and reporting programming language. The data set was normalized using the "limma" package of R software, and Wilcoxon tests were employed (* $p<0.05$ and ** $p<0.01$). The ggplot2 data package was utilized to standardize the microarray data from the GSE49543 dataset, identifying differential genes. Subsequently, we employed Sangerbox, a web-based platform for clinical health analysis (http://vip.sangerbox.com) [13], to generate a volcano plot.

Differential expression analysis of mitochondria-related genes

The intersection genes between the identified differentially expressed genes and mitochondrial genes were selected. A Venn diagram was generated using the "VennDiagram package" in R software to visually represent the number of differentially expressed mitochondria-related genes associated with ARHL.

Construction of PPI network and identification of hub gene

The Protein-Protein Interaction Networks (PPI) were constructed using the STRING online database (https://cn.string-db.org/) [14]. Through the utilization of Cytosc ape (https://www.statistical-analysis.top/Cytoscape) [15, 16], a software for biological network analysis and visualization, we performed an analysis on CytoHubba MCC to identify the top 10 genes in the PPI network, which were determined as key genes: Fdx1, Mrpl24 Mtif2, Arg2, Aco2 Ndufs1, Bcs1l, Ndufaf5, Nsun2, Sdhaf1.

Cell line

In this experiment, the mouse cochlea hair cell immortal HEI-OC1 cell line, purchased from Ubigene Company, was cultured in Dulbecco's modified Eagle's culture medium (DMEM) (Gibco, USA) under humid conditions with 5% CO2 at 37℃. The culture medium was supplemented with 10% fetal bovine serum (FBS) (ExCell, CHINA) and 100 U/ml penicillin/streptomycin (Gibco, USA). They were treated with D-galactose (Solebol, China) at a 30 mg/ml concentration for 72 h to induce ageing in the cells.

Western blot

HEI-OC1 cells were lysed with RIPA buffer containing PMSF and protease inhibitor, and the protein concentration was determined using the BCA method. 20 μg of protein were separated by 12% SDS-PAGE and transferred onto a PVDF membrane, followed by overnight incubation with specific primary antibodies at 4℃. Immunoreactive bands were detected using chemiluminescence. Antibodies used included anti-ACO2 (proteintech, China, Cat No. 11134-1-AP), anti-BCS1L (proteintech, China, Cat No. 60212-1-Ig), anti-NDUSF1 (proteintech, China, Cat No. 12444-1-AP), and anti-GAPDH (proteintech, China, Cat No. 10494-1-AP). The three bands of each group shown in the image were taken from three tissue samples.

Immunofluorescence

The cells were seeded onto small glass slides and subjected to the corresponding treatments. After fixation with 4% PFA for 30 min, permeabilization was achieved by incubating the cells with 0.5% Triton X-100 for 30 min. Subsequently, blocking was performed using 5% BSA for 1 h. The cells were then incubated overnight at 4℃ with the primary antibody specific to their target protein. The following day, fluorescently labelled secondary antibodies and DAPI were applied to stain the nuclei of the cells. Finally, immunofluorescence analysis was conducted under a fluorescence microscope.

Statistical analysis

The statistical analysis was conducted using GraphPad Prism 8.0 software. Data were presented as mean ± standard error of the mean (SEM). Comparison between the two groups was performed using an unpaired, two-tailed Student's t-test. A significance level of $P<0.05$ indicated statistical significance (*=$P<0.05$, **=$P<0.01$, ***=$P<0.001$), and NS = no statistically significant difference between the groups.

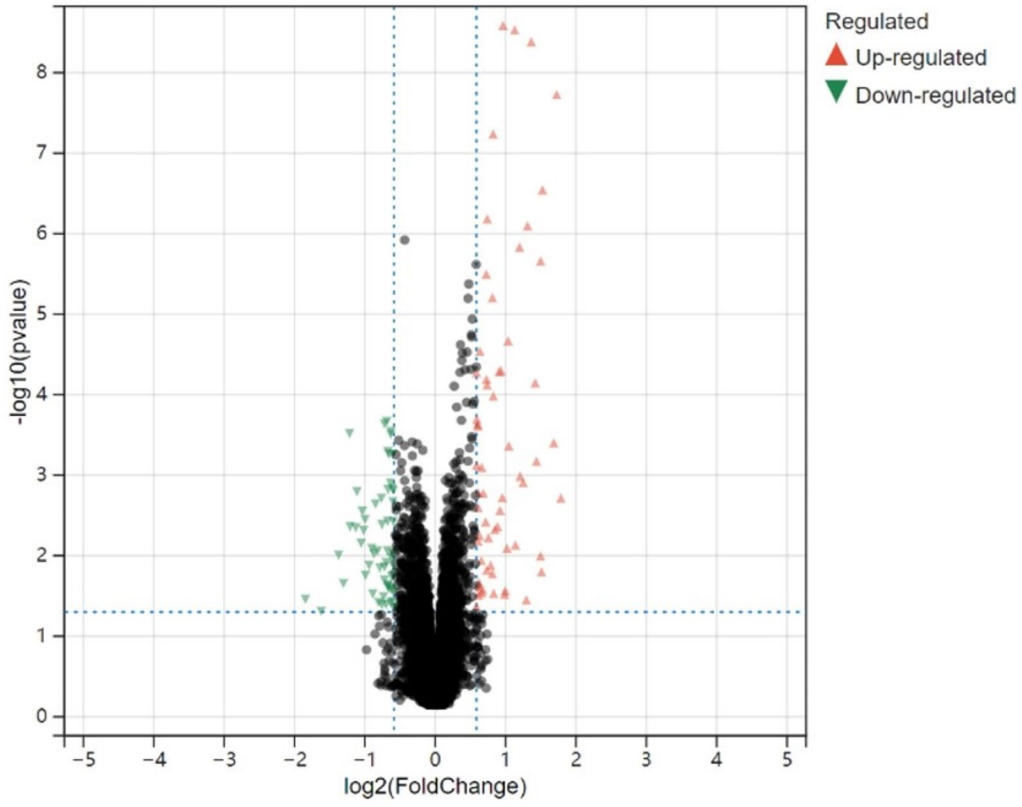

Fig. 2 Differentially expressed genes in ARHL. Volcano map of differentially expressed genes in ARHL obtained through database analysis

Table 1 GO analysis: Biological Processes (Top 10)

ONTOLOGY	Description	P. Value
BP	mitochondrial respiratory chain complex assembly	2.48×10^{-8}
BP	mitochondrial gene expression	1.58×10^{-5}
BP	small molecule catabolic process	1.63×10^{-5}
BP	NADH dehydrogenase complex assembly	2.16×10^{-5}
BP	mitochondrial respiratory chain complex I assembly	2.16×10^{-5}
BP	carboxylic acid catabolic process	5.52×10^{-5}
BP	organic acid catabolic process	5.71×10^{-5}
BP	generation of precursor metabolites and energy	6.32×10^{-5}
BP	mitochondrial transmembrane transport	6.56×10^{-5}
BP	reactive oxygen species metabolic process	7.54×10^{-5}

Results

A total of 503 differentially expressed genes associated with ARHL were identified

A total of 503 differentially expressed genes (ARHL-DEGs) were identified using the R language package "limma (v3.48.3)"(Fig. 2). 233 genes exhibited upregulation with a conditional logFC > 0 threshold, while 270 genes showed downregulation with a logFC < 0 threshold.

The enrichment analysis of differentially expressed genes showed that the mitochondrial function had changed significantly. The clusterProfiler software package was utilized to analyze the differential gene expression in ARHL, resulting in 659 significant GO terms(https://geneontology.org/) [17, 18] and 35 KEGG pathways ((https://www.genome.jp/kegg/) ($p < 0.05$) [19]. The identified biological processes involve multiple mitochondrial functions such as mitochondrial respiratory chain complex assembly, NADH dehydrogenase complex assembly, mitochondrial transmembrane transport, and reactive oxygen species metabolic process (Table 1). Cellular components are also involved in the composition of mitochondria, including integral components of

Table 2 GO analysis: Cellular Components (Top 10)

ONTOLOGY	Description	P. Value
CC	integral component of mitochondrial membrane	6.67×10^{-5}
CC	intrinsic component of mitochondrial membrane	7.17×10^{-5}
CC	mitochondrial matrix	0.000177148
CC	integral component of mitochondrial inner membrane	0.001041753
CC	intrinsic component of mitochondrial inner membrane	0.001084508
CC	myelin sheath	0.001170597
CC	extracellular exosome	0.004590626
CC	integral component of organelle membrane	0.005758767
CC	extracellular vesicle	0.005771183
CC	extracellular organelle	0.006661356

Table 3 GO analysis: Molecular Function (Top 10)

ONTOLOGY	Description	P. Value
MF	iron-sulfur cluster binding	3.37×10^{-5}
MF	metal cluster binding	3.37×10^{-5}
MF	mRNA methyltransferase activity	4.76×10^{-5}
MF	catalytic activity, acting on a tRNA	0.000209712
MF	2 iron, 2 sulfur cluster binding	0.000278844
MF	tRNA methyltransferase activity	0.00045116
MF	carboxylic ester hydrolase activity	0.000544873
MF	4 iron, 4 sulfur cluster binding	0.000630939
MF	lyase activity	0.000850064
MF	methyltransferase activity	0.000900898

Table 4 KEGG enrichment pathway analysis (Top 10)

ID	Description	P. Value
mmu00330	Arginine and proline metabolism - Mus musculus (house mouse)	7.75×10^{-5}
mmu01230	Biosynthesis of amino acids - Mus musculus (house mouse)	0.000241277
mmu00220	Arginine biosynthesis - Mus musculus (house mouse)	0.000443612
mmu01040	Biosynthesis of unsaturated fatty acids - Mus musculus (house mouse)	0.00129304
mmu01210	2-Oxocarboxylic acid metabolism - Mus musculus (house mouse)	0.00129304
mmu00310	Lysine degradation - Mus musculus (house mouse)	0.004520092
mmu04146	Peroxisome - Mus musculus (house mouse)	0.008212206
mmu01200	Carbon metabolism - Mus musculus (house mouse)	0.015447104
mmu00120	Primary bile acid biosynthesis - Mus musculus (house mouse)	0.028344546
mmu00770	Pantothenate and CoA biosynthesis - Mus musculus (house mouse)	0.032995091

the mitochondrial membrane and mitochondrial matrix (Table 2). Molecular functions involve energy metabolism within mitochondria, such as iron-sulfur cluster binding and 4-sulfur cluster binding (Table 3). KEGG pathway analysis revealed involvement in the biosynthesis of amino acids, biosynthesis of unsaturated fatty acids and carbon metabolism (Table 4). At the same time, it is widely acknowledged that mitochondria play a crucial role in carbohydrate, amino acid, and lipid metabolism.

A total of 28 mitochondrial genes were differentially expressed

We observed a strong association between gene enrichment results and mitochondria. Thus, we integrated these 503 differential genes with mitochondrial genes to identify the differentially expressed genes related to mitochondria. A total of 28 differentially expressed mitochondrial genes associated with ARHL were analyzed using the Venn mapping software package (1.7.1) (Fig. 3A). A hypergeometric test was performed on the dataset, yielding a p-value of 0.004122179, which indicates statistical significance.

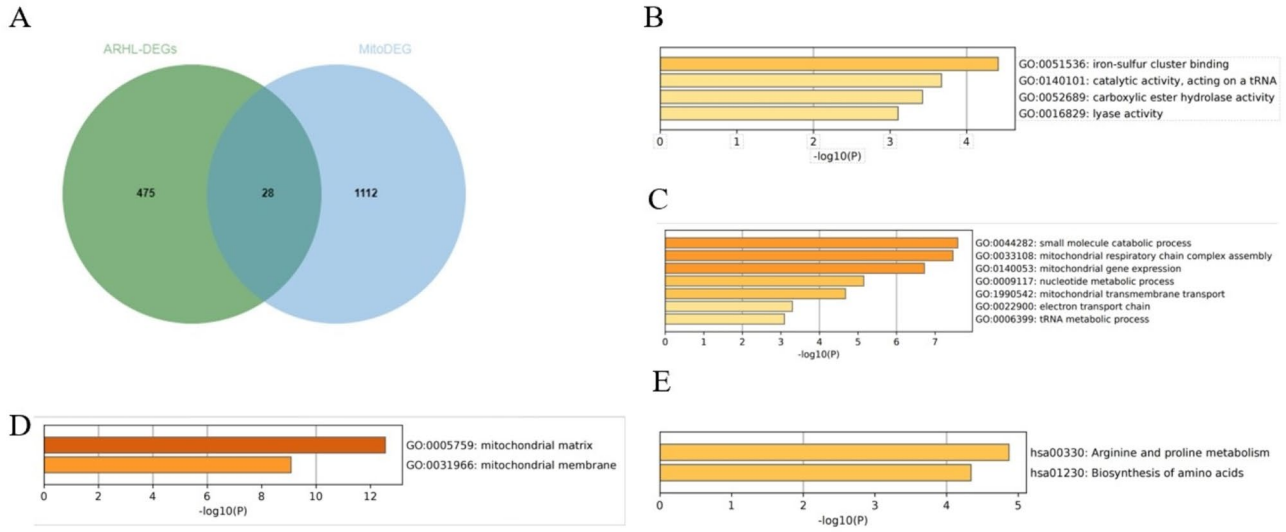

Fig. 3 28 differentially expressed mitochondrial genes were found. **A**. The differentially expressed genes in ARHL interacted with mitochondrial genes, resulting in the identification of 28 differentially expressed mitochondrial genes. **B**-**D**, GO analysis was performed on the differentially expressed mitochondrial genes, leading to the enrichment results of molecular functions, biological processes, and cell components. **E**. Pathway results were obtained through KEGG enrichment

The Metascape tool was utilized to perform enrichment analysis on these 28 differentially expressed mitochondrial genes, using the following criteria: Min Overlap ≤ 3, P-Value Cutoff ≤ 0.01, and Min Enrichment ≤ 1.5(http://metascape.org/gp/index.html#/main/step1) [20, 21]. The results were visualized in a bar chart. We observed that NDUFS1, FDX1, ACO2, ALDH2, NDUFAF5, HSD17B4 and AASS were significantly enriched in iron-sulfur cluster binding at the molecular function. Additionally, ALDH2, ACOT7 and ABHD10 exhibited enrichment in catalytic activity, acting on a tRNA. METTL8, NSUN2, NDUFAF5 and GARS1 showed enrichment in carboxylic ester hydrolase activity while CLYBL, ACO2 and HSD17B4 demonstrated enrichment in lyase activity (Fig. 3B). In terms of biological processes, GTP2, ARG2, AASS, HSD17B4, AcoT7, ALDH2, NUDT5 and GARS1 are involved in small molecule catabolic process. NDUFAF5, NDUFS1, BCS1L, SLC25A33, SDHAF1 and RHOT1 contribute to the assembly of the mitochondrial respiratory chain complex assembly. ACOT7, HSD17B4, AASS, NDUFS1, NUDT5, GARS1 and CKMT1B play a role in mitochondrial gene expression. SLC25A33, SFXN1, SFXN4 and RHOT participate in nucleotide metabolism. ALDH2, FDX1, ACO2 and NDUFS participate in the electron transport chain; METTL8, NSUN2, GARS and NDUFAF5 are involved in tRNA metabolism (Fig. 3C). In terms of cell components, SDHAF1 MRPL24, NDUFS1, ARG2, GARS1, GPT2, FDX1, ABHD10, AASS, ALDH2, AC02 participated in the composition of mitochondrial membrane. NDUFS1, MRPL24, BCS1L, SLC25A33, SFXN1, NDUFAF5, CKMT1B, SFXN4, RHOT1 SLC30A9 participate in the formation of mitochondrial matrix (Fig. 3D). KEGG analysis showed that ALDH2, CKMT1B and ARG2 were involved in arginine and proline metabolic pathways. ARG2, AC02 and GPT2 participate in the metabolic pathway of amino acids (Fig. 3E).

Three crucial mitochondrial genes were identified

A network diagram depicting protein interactions of differentially expressed mitochondrial genes was constructed using the STRING database. Subsequently, a network clustering module comprising 28 nodes and 17 edges was obtained (Fig. 4A). Next, Cytoscape's CytoHubba MCC software plugin was employed for analysis, identifying ten top hub genes. Among them are Aco2, Bcs1l and Ndufs1, which occupy central positions within the module and serve as hub genes associated with ARHL (Fig. 4B). Furthermore, the expression levels of these three hub genes exhibit significant downregulation in ARHL.

The expression of Aco2, Bcs1l and Ndufs1 decreased in senescent hair cells

In order to validate the conclusion derived from the aforementioned analysis, we conducted cell experiments to corroborate it. Specifically, we performed in vitro experiments using the hair cell immortal cell line HEI-OC1. We exposed the cells to D-galactose at a concentration of 30 mg/ml for 72 h to simulate senescent hair cells [22]. Subsequently, we assessed the levels of three hub genes through immunofluorescence and Western blot. Our findings revealed a significant downregulation in the expression levels of Aco2, Bcs1l, and Ndufs1 in aging hair

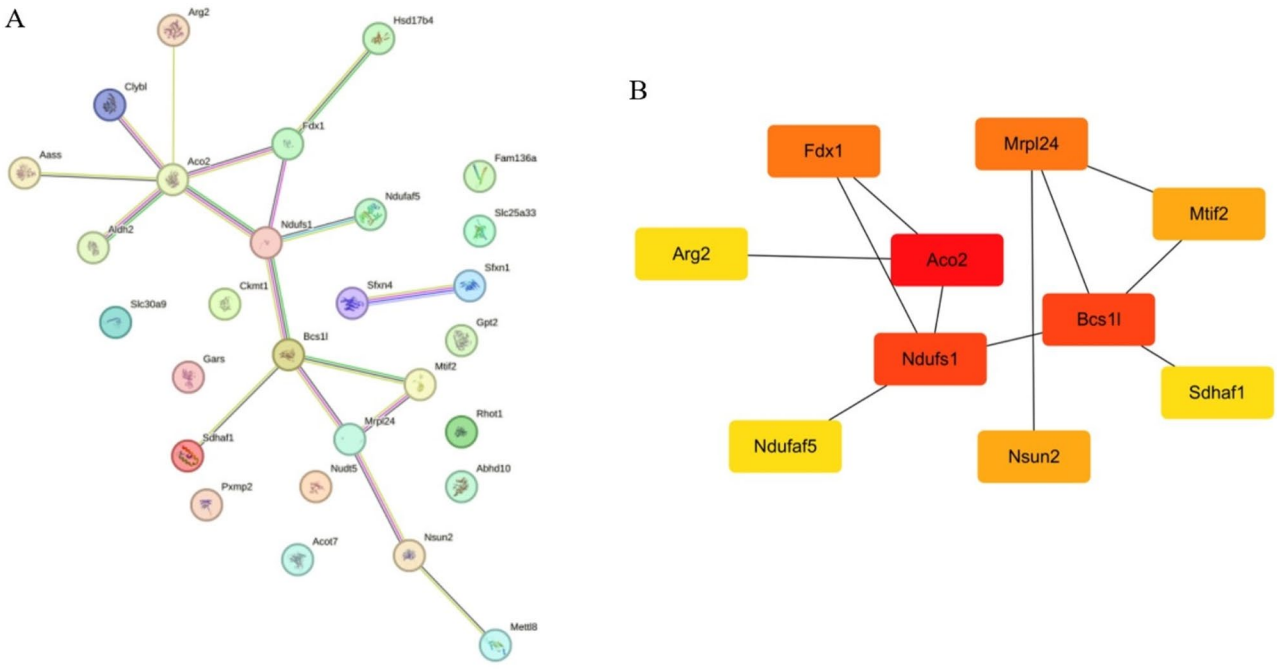

Fig. 4 A total of 10 pivotal genes and 3 hub genes were identified. **A**. PPI network analysis chart. **B**. Identify 10 pivotal genes, among which aco2, ndufs1 and bcs1l are hub genes

cells compared to the control group in both immunofluorescence (ACO2, $P = 0.0004$; NDUFS1, $P = 0.0017$; BCS1L, $P = 0.0011$) and Western blot ((ACO2, $P = 0.0053$; BCS1L, $P = 0.0006$; NDUFS1, $P = 0.0047$) (Fig. 5).

Discussion

According to previous speculation, age-related hearing loss is primarily attributed to the degeneration of stria vascularis (SV), which plays a crucial role in maintaining the electrical potential of the inner ear and facilitating the conversion of mechanical signals into electrical signals in the cochlea [23]. Recent research has identified that cochlear hair cells (HC) are pivotal in determining ARHL. In their autopsy study involving 120 cadaver patients, Liberman et al. observed a significant correlation between hair cell loss and the extent of hearing damage. At the same time, stria vascularis were found to be unrelated to hearing damage levels. This groundbreaking study provided novel insights into the key component responsible for ARHL within the human cochlea [24].

Cochlear hair cells are highly energy-consuming cells, primarily relying on the oxidative phosphorylation process of mitochondria for their energy source [4, 25]. Mitochondria in hair cells maintain homeostasis, thereby ensuring normal mitochondrial function. In hair cells, mitochondria play a crucial role in regulating oxidative metabolism and generating Reactive Oxygen Species (ROS). The aging of hair cells is characterized by the accumulation of oxidative damage caused by ROS buildup, with mitochondria being the primary site of ROS-induced cellular damage [26, 27]. Additionally, mitochondria are involved in various other processes, such as signaling, cell differentiation, and regulation of the cell cycle and growth [28, 29]. During the aging process of cochlear hair cells, disturbances in mitochondrial homeostasis lead to mitochondrial dysfunction (MD), resulting in alterations in intracellular redox levels and subsequent cell death [30].

The human mitochondrial genome is a circular, double-stranded, supercoiled molecule with one to several thousand copies per cell consisting of 16,569 bases [31]. Although proteins also protect mitochondrial genes, their protective effect is significantly weaker than nuclear genes, rendering them more susceptible to external genotoxic substances [32]. Accumulation of ROS in hair cells also induces mutations in the mitochondrial genome, leading to damage in mitochondrial genes. Mutation and deletion of mitochondrial genes play a crucial role in hair cell senescence. Markaryan et al. discovered that cochlear tissues from elderly humans exhibited deficiency in 4977-bp mitochondria, and the probability of deficiency would increase with age [33]. Enhanced protection of mitochondrial genes could be beneficial. Jun Li et al. utilized the DNA methylation inhibitor 5-azacytidine to reduce the methylation level of SOD2, thereby decreasing oxidative stress and copy number variations (CNVs) of mitochondrial gene 4834 mutations while inhibiting H2O2-induced apoptosis in hair cells [34]. Subsequently, more studies have confirmed the close association between mutation and deletion of mitochondrial genes

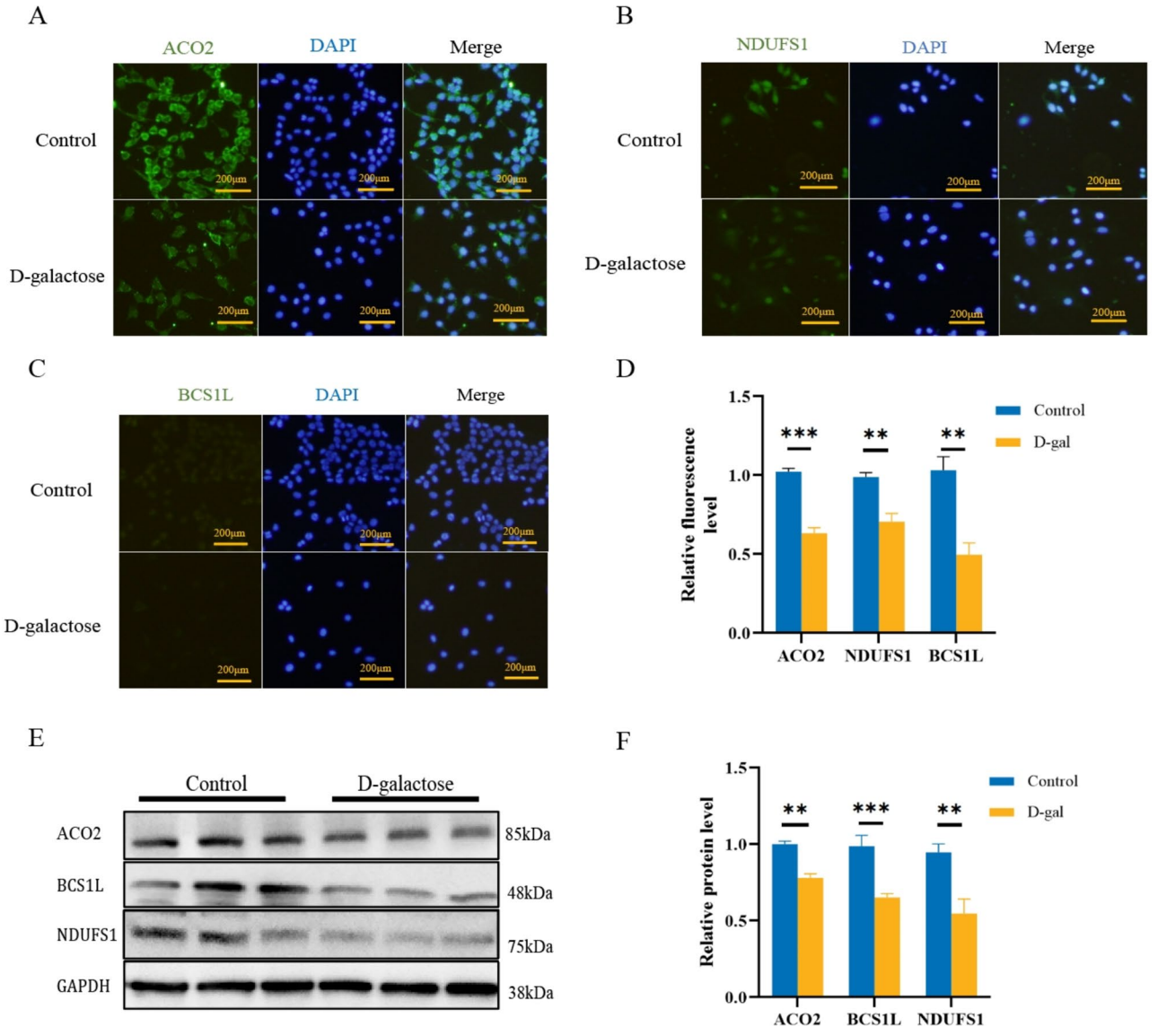

Fig. 5 The level of ACO2, NDUFS1 and BCS1L in aging hair cells are downregulated. **A**-**C**. results of immunofluorescence. **D**. Statistical analysis of the average fluorescence intensity of fluorescent staining. **E**-**F**. Results of Western blot.Full-length blots/gels are presented in Supplementary Figure 1-4. Data were presented as mean ±SEM. A significance level of $P < 0.05$ indicated statistical significance (* = $P < 0.05$, ** = $P < 0.01$, *** = $P < 0.001$), and NS = no statistically significant differencebetween the groups

with age-related hearing loss (ARHL), suggesting an increased risk for ARHL due to its mutation [35].

A total of 503 DEGs were identified. KEGG pathway enrichment analysis revealed significant enrichment of DEGs in the oxidative phosphorylation signaling pathway, amino acid anabolic signaling pathway, ribosome signaling pathway, peroxisome signaling pathway, and other pathways associated with mitochondrial function. These findings suggest that alterations in these signaling pathways may contribute to mitochondrial dysfunction and subsequently induce ARHL. Following the GO functional enrichment analysis of DEGs, Tables present the top ten entries for each of the three GO ontologies. BP primarily encompasses processes related to mitochondrial transmembrane transport, metabolic processes involving reactive oxygen species, assembly of mitochondrial respiratory chain complexes and gene expression within mitochondria, NADH dehydrogenase complex assembly, precursor metabolite and energy production, as well as organic acid decomposition and small molecule metabolism. CC involves forming components such as mitochondrial membranes, mitochondrial matrixes, myelin sheaths, extracellular exosomes, and complete components found in other organelle membranes, including extracellular vesicles and organelles. MM molecules bind to 2- and 4-ferric sulfur clusters or

metal clusters, mRNA/tRNA methyltransferase activity, catalytic activity, and carboxylic ester hydrolase activity. The DEGs in ARHL have consistently been a critical focus in the investigation of presbycusis. Previous studies have examined DEGs in the cochlea. Yang et al. analysed cochlear hair cells, auditory nerves, and SV datasets to identify genes differentially expressed across these three cochlear components [36]. Given that hair cells are considered pivotal in the pathogenesis of ARHL and considering the significant role mitochondria play in hair cell death, our research targets explicitly mitochondria-related genes in cochlear hair cells.

Given the strong correlation between these differential genes and mitochondrial function, we performed an intersection analysis with mitochondria-related genes to identify differentially expressed mitochondria-related genes associated with age-related hearing loss. Aco2, Bcs1l, and Ndufs1 emerged as three key hub genes closely linked to mitochondrial function.

Mitochondrial aconitase 2 (ACO2) belongs to the iron-sulfur cluster hydratase family. Upon binding to the enzyme structure, the active iron-sulfur cluster reverses citric acid into isocitrate in the TCA cycle and facilitates dehydration and rehydration reactions [37]. Aco2 is an indispensable enzyme in the tricarboxylic acid cycle, which is crucial in coordinating mitochondrial and autophagy functions for energy metabolism within the cellular mitochondrial respiratory chain. ACO2 significantly contributes to cellular energy metabolism, maintenance of iron homeostasis, resistance against oxidative stress, and preservation of mitochondria-related gene integrity [38]. Research has indicated that mutations in the ACO2 gene may be associated with premature aging [39]. Furthermore, studies have demonstrated that ACO2 impacts neuronal function and survival during the aging process, potentially contributing to Alzheimer's disease onset [40]. Targeting ACO2 to enhance energy metabolism could serve as a promising therapeutic strategy for Parkinson's disease and other neurodegenerative disorders [41]. Currently, there are extensive reports on the involvement of ACO2 mutations in energy metabolism issues and the progression of neurodegenerative diseases such as optic atrophy, microcephaly, intellectual impairment, cognitive decline, hypotonia spastic paraplegia [42–44].

As a chaperone and translocation enzyme in the inner mitochondrial membrane, the BCS1L protein plays a crucial role in promoting the final folding and assembly of respiratory complex III by facilitating the insertion of the Rieske iron-sulfur subunit into the complex [45]. The functional structure of BCS1L consists of three distinct domains: (a) N-terminal domain comprising three unique parts - transmembrane domain (TMD), mitochondrial targeting sequence (MTS), and input auxiliary sequence (IAS); (b) BSC1L-specific domain; and (c) C-terminal AAA-ATPase domain. The interactions between TMD/MTS and BCS1L assist in anchoring proteins within the mitochondrial matrix for subsequent transport [46, 47]. Mutations in BCS1L are commonly associated with defects in human mitochondrial complex III [48], where mutated BCS1L protein disrupts complex III assembly, reduces mitochondrial electron transport chain activity, impairs ATP synthesis, and increases reactive oxygen species production [49], thereby causing damage to cellular components that accelerate aging. In addition to various diseases such as sensorineural hearing loss (Bjornstad syndrome) and severe multisystem organ failure (Complex III deficiency and GRACILE syndrome), mutations in BCS1L also lead to features related to central nervous system dysfunction, including movement disorders, seizures, and clinical manifestations resembling Leigh's encephalopathy [50]. Furthermore, BCS1L regulates mitochondrial autophagy; its dysfunction affects damaged mitochondria clearance, leading to dysfunctional organelle accumulation, which can contribute to cell senescence [45].

NADH: ubiquinone oxidoreductase core subunit S1 (NDUFS1) is the largest subunit within mitochondrial complex I, responsible for catalyzing the initial step of respiratory nicotinamide adenine dinucleotide (NADH) oxidation in mitochondria. It plays a pivotal role in maintaining the stability and functionality of mitochondrial complex I [51]. Deletion or mutation of NDUFS1 results in reduced levels and catalytic activity of mitochondrial complex I, disrupting NADH homeostasis and impeding electron transfer within the respiratory chain. Consequently, this leads to substantial intracellular reactive oxygen species (ROS) production [52], impaired mitochondrial function, and ultimately accelerates cellular aging processes. Furthermore, deficiency in NDUFS1 causes loss of mitochondrial complex I, contributing to Leigh encephalopathy [53]. Additionally, studies have suggested that mutations in Ndufs1 may be associated with Parkinson's disease and can serve as diagnostic markers for its detection [54]. A Danish cohort study has also demonstrated that NDUFS1 reflects physical conditions among elderly individuals by correlating with grip strength and walking speed [55].

Conclusion

This study identified 503 differentially expressed genes in age-related hearing loss using bioinformatics tools. Among them, 28 differentially expressed mitochondria-related genes were further associated with the mitochondrial function database. Subsequently, three hub genes (Aco2, Bcs1l, and Ndufs1) involved in mitochondrial function injury were discovered. The expression of these three genes was found to be decreased in the hair cells

of ARHL. Investigating the role of ACO2, BCS1L, and NDUFS1 in the ARHL process is crucial for understanding its mechanism and developing related therapeutic approaches. The integrity of mitochondrial function and disruption of homeostasis are important mechanisms underlying hair cell senescence and play a significant role in the occurrence and progression of age-related hearing loss. This study provides valuable insights into the pathogenesis of ARHL and offers an important target for understanding its pathogenesis and developing treatment strategies.

Supplementary Information

The online version contains supplementary material available at https://doi.org/10.1186/s12864-025-11287-5 .

Supplementary Material 1

Supplementary Material 2

Supplementary Material 3

Supplementary Material 4

Supplementary Material 5

Supplementary Material 6

Supplementary Material 7

Acknowledgements
Not applicable.

Author contributions
THZ is the corresponding author, and she contributes to the conception of the study. TYM contributes to design. XYZ complete the bioinformatics analysis. MTL and SJX contribute to the experiment in vitro. YYW and QLW contribute to data analysis and interpretation. All authors contributes to the writing of the manuscript.

Funding
Tianyu Ma receives the Heilongjiang Provincial Nature Foundation (YQ2022H013) and Innovation Program of the First Hospital of Harbin Medical University. Mengting Liu receives funding from Postdoctoral Program in Heilongjiang Province (LBH-Z23220) and Innovation Program of Harbin Medical University. Tianhong Zhang receives funding from Key Research and Development program of Heilongjiang Province (2023ZX06C07).

Data availability
The datasets generated and/or analysed during the current study are available in the GEO public database (https://www.ncbi.nlm.nih.gov/geo/query/acc.cgi?acc=GSE49543) and Mouse MitoCarta 3.0 database (https://personal.broadinstitute.org/scalvo/MitoCarta3.0/mouse.mitocarta3.0.html). The data that support the findings of this study are available from the corresponding author upon reasonable request.

Declarations

Ethics approval and consent to participate
Not applicable.

Consent for publication
Not applicable.

Competing interests
The authors declare no competing interests.

Received: 23 May 2024 / Accepted: 23 January 2025
Published online: 05 March 2025

References

1. Hearing loss prevalence and years lived with disability, 1990–2019: findings from the global burden of Disease Study 2019. Lancet, 2021. 397(10278): pp. 996–1009.
2. Tarawneh HY, et al. Understanding the Relationship between Age-related hearing loss and Alzheimer's Disease: a narrative review. J Alzheimers Dis Rep. 2022;6(1):539–56.
3. Elliott KL, et al. Age-related hearing loss: sensory and neural etiology and their interdependence. Front Aging Neurosci. 2022;14:814528.
4. Tan WJT, Song L. Role of mitochondrial dysfunction and oxidative stress in sensorineural hearing loss. Hear Res. 2023;434:108783.
5. Willems PH, et al. Redox Homeostasis and mitochondrial dynamics. Cell Metab. 2015;22(2):207–18.
6. Falah M, et al. Expression levels of the BAK1 and BCL2 genes highlight the role of apoptosis in age-related hearing impairment. Clin Interv Aging. 2016;11:1003–8.
7. Andrade B et al. The relationship between reactive oxygen species and the cGAS/STING signaling pathway in the inflammaging process. Int J Mol Sci, 2022. 23(23).
8. Stenberg S et al. Genetically controlled mtDNA deletions prevent ROS damage by arresting oxidative phosphorylation. Elife, 2022. 11.
9. Yang L, et al. NAD(+) dependent UPR(mt) activation underlies intestinal aging caused by mitochondrial DNA mutations. Nat Commun. 2024;15(1):546.
10. Shoffner JM, et al. Spontaneous Kearns-Sayre/chronic external ophthalmoplegia plus syndrome associated with a mitochondrial DNA deletion: a slip-replication model and metabolic therapy. Proc Natl Acad Sci U S A. 1989;86(20):7952–6.
11. Clough E, Barrett T. The Gene expression Omnibus Database. Methods Mol Biol. 2016;1418:93–110.
12. Rath S, et al. MitoCarta3.0: an updated mitochondrial proteome now with sub-organelle localization and pathway annotations. Nucleic Acids Res. 2021;49(D1):D1541–7.
13. Shen W, et al. Sangerbox: a comprehensive, interaction-friendly clinical bioinformatics analysis platform. iMeta. 2022;1(3):e36.
14. Szklarczyk D, et al. The STRING database in 2021: customizable protein-protein networks, and functional characterization of user-uploaded gene/measurement sets. Nucleic Acids Res. 2021;49(D1):D605–12.
15. Shannon P, et al. Cytoscape: a software environment for integrated models of biomolecular interaction networks. Genome Res. 2003;13(11):2498–504.
16. Otasek D, et al. Cytoscape automation: empowering workflow-based network analysis. Genome Biol. 2019;20(1):185.
17. Ashburner M, et al. Gene ontology: tool for the unification of biology. The Gene Ontology Consortium. Nat Genet. 2000;25(1):25–9.
18. Aleksander SA et al. The Gene Ontology knowledgebase in 2023. Genetics, 2023. 224(1).
19. Kanehisa M, et al. KEGG for taxonomy-based analysis of pathways and genomes. Nucleic Acids Res. 2023;51(D1):D587–92.
20. Subramanian A, et al. Gene set enrichment analysis: a knowledge-based approach for interpreting genome-wide expression profiles. Proc Natl Acad Sci U S A. 2005;102(43):15545–50.
21. Zhou Y, et al. Metascape provides a biologist-oriented resource for the analysis of systems-level datasets. Nat Commun. 2019;10(1):1523.
22. He W, et al. Promoting TFEB nuclear localization with curcumin analog C1 attenuates sensory hair cell injury and delays age-related hearing loss in C57BL/6 mice. Neurotoxicology. 2023;95:218–31.
23. Carraro M, Harrison RV. Degeneration of stria vascularis in age-related hearing loss; a corrosion cast study in a mouse model. Acta Otolaryngol. 2016;136(4):385–90.
24. Wu PZ, et al. Age-related hearing loss is dominated by damage to inner ear sensory cells, not the Cellular Battery that Powers them. J Neurosci. 2020;40(33):6357–66.
25. Puschner B, Schacht J. Energy metabolism in cochlear outer hair cells in vitro. Hear Res. 1997;114(1–2):102–6.
26. Lyu AR et al. Mitochondrial damage and necroptosis in Aging Cochlea. Int J Mol Sci, 2020. 21(7).
27. Zhang Y, et al. Increased mitophagy protects cochlear hair cells from aminoglycoside-induced damage. Autophagy. 2023;19(1):75–91.

28. Sykes DB. The emergence of dihydroorotate dehydrogenase (DHODH) as a therapeutic target in acute myeloid leukemia. Expert Opin Ther Targets. 2018;22(11):893–8.
29. Anand R, et al. The i-AAA protease YME1L and OMA1 cleave OPA1 to balance mitochondrial fusion and fission. J Cell Biol. 2014;204(6):919–29.
30. Huang S, et al. Baicalein inhibits SARS-CoV-2/VSV replication with interfering mitochondrial oxidative phosphorylation in a mPTP dependent manner. Signal Transduct Target Ther. 2020;5(1):266.
31. Yan C et al. Mitochondrial DNA: distribution, mutations, and elimination. Cells, 2019. 8(4).
32. Yamauchi S, et al. Mitochondrial fatty acid oxidation drives senescence. Sci Adv. 2024;10(43):eado5887.
33. Markaryan A, Nelson EG, Hinojosa R. Quantification of the mitochondrial DNA common deletion in presbycusis. Laryngoscope. 2009;119(6):1184–9.
34. Li J, et al. Effect of SOD2 methylation on mitochondrial DNA4834-bp deletion mutation in marginal cells under oxidative stress. Bosn J Basic Med Sci. 2020;20(1):70–7.
35. Scarpelli M, et al. Mitochondrial sensorineural hearing loss: a retrospective study and a description of Cochlear Implantation in a MELAS patient. Genet Res Int. 2012;2012:287432.
36. Yang X, et al. Key genes and potential drugs in age-related hearing loss: transcriptome analysis of cochlear hair cells in old mice. Cell Mol Biol (Noisy-le-grand). 2023;69(6):67–74.
37. Cheng Z, et al. Impaired energy metabolism in a Drosophila model of mitochondrial aconitase deficiency. Biochem Biophys Res Commun. 2013;433(1):145–50.
38. Chen Y, et al. Mitochondrial aconitase controls adipogenesis through mediation of cellular ATP production. Faseb j. 2020;34(5):6688–702.
39. Poon HF, et al. Proteomics analysis provides insight into caloric restriction mediated oxidation and expression of brain proteins associated with age-related impaired cellular processes: mitochondrial dysfunction, glutamate dysregulation and impaired protein synthesis. Neurobiol Aging. 2006;27(7):1020–34.
40. Mangialasche F, et al. Lymphocytic mitochondrial aconitase activity is reduced in Alzheimer's disease and mild cognitive impairment. J Alzheimers Dis. 2015;44(2):649–60.
41. Zhu J, et al. ACO2 deficiency increases vulnerability to Parkinson's disease via dysregulating mitochondrial function and histone acetylation-mediated transcription of autophagy genes. Commun Biol. 2023;6(1):1201.
42. Neumann MA, et al. Haploinsufficiency due to a novel ACO2 deletion causes mitochondrial dysfunction in fibroblasts from a patient with dominant optic nerve atrophy. Sci Rep. 2020;10(1):16736.
43. Park JS, et al. Novel compound heterozygous ACO2 mutations in an infant with progressive encephalopathy: a newly identified neurometabolic syndrome. Brain Dev. 2020;42(9):680–5.
44. Charif M, et al. Dominant ACO2 mutations are a frequent cause of isolated optic atrophy. Brain Commun. 2021;3(2):fcab063.
45. Morán M, et al. Cellular pathophysiological consequences of BCS1L mutations in mitochondrial complex III enzyme deficiency. Hum Mutat. 2010;31(8):930–41.
46. Baker RA, et al. Clinical spectrum of BCS1L mitopathies and their underlying structural relationships. Am J Med Genet A. 2019;179(3):373–80.
47. Stan T, et al. Mitochondrial protein import: recognition of internal import signals of BCS1 by the TOM complex. Mol Cell Biol. 2003;23(7):2239–50.
48. Brischigliaro M, et al. Modelling of BCS1L-related human mitochondrial disease in Drosophila melanogaster. J Mol Med (Berl). 2021;99(10):1471–85.
49. Hinson JT, et al. Missense mutations in the BCS1L gene as a cause of the Björnstad syndrome. N Engl J Med. 2007;356(8):809–19.
50. Hikmat O, et al. Expanding the phenotypic spectrum of BCS1L-related mitochondrial disease. Ann Clin Transl Neurol. 2021;8(11):2155–65.
51. Hirst J. Mitochondrial complex I. Annu Rev Biochem. 2013;82:551–75.
52. Hoefs SJ, et al. Novel mutations in the NDUFS1 gene cause low residual activities in human complex I deficiencies. Mol Genet Metab. 2010;100(3):251–6.
53. Tuppen HA, et al. The p.M292T NDUFS2 mutation causes complex I-deficient Leigh syndrome in multiple families. Brain. 2010;133(10):2952–63.
54. Chi J, et al. Integrated Analysis and Identification of Novel biomarkers in Parkinson's Disease. Front Aging Neurosci. 2018;10:178.
55. Dato S, et al. Contribution of genetic polymorphisms on functional status at very old age: a gene-based analysis of 38 genes (311 SNPs) in the oxidative stress pathway. Exp Gerontol. 2014;52:23–9.

Publisher's note